

Electronic supporting information

A novel Kolbe reaction pathway for a selective one- and two-electron reduction of azo compounds

Wen-Fu Fu,^{*a,b} Huifang-Jie Li,^a De-Hui Wang,^b Liang-Jun Zhou,^b Li Li,^a Xin Gan,^b Quan-Qing Xu^b and Hai-Bin Song^c

^a Key Laboratory of Photochemical Conversion and Optoelectronic Materials, TIPC CAS, Technical Institute of Physics and Chemistry, Chinese Academy of Sciences, Peking, 100190, P.R. China.

^b College of Chemistry and Chemical Engineering, Yunnan Normal University, Kunming, 650092, P.R. China.

^c Department of Chemistry, The State Key Laboratory of Elemento-Organic Chemistry, Nankai University, Tianjin, 300071, P.R. China.

Experimental Sections

1. Materials and methods

General methods: ^1H NMR and ^{13}C NMR spectra were measured either on Bruker DMX-300 (300 MHz), Bruker DPX-400 (400 MHz) or Bruker AV-500 (500 MHz) at 298K with chemical shifts (δ , ppm) relative to tetramethylsilane (Me_4Si) for ^1H . Elemental analysis was carried out with a Carlo Erba 1106 element analysis instrument. The UV-Vis spectra were taken on a HITACHI U-3010 spectrophotometer. Mass spectra were recorded on BIFLEX-III MALDI-TOF mass spectrometer for Matrix-assisted laser desorption (MALDI) and Finnigan GC-MS 4021 mass spectrometer for EI. IR data were recorded on a Varian 3100 FTIR spectrometer. All chemicals for the synthesis were purchased from commercial suppliers and solvents (HPLC) were purified according to standard procedures. Column chromatography was performed on Al_2O_3 (100-200 mesh).

Experimental procedure for X-ray crystallographic analysis: Crystals of **L**, **H₂L**, **1** and **2** suitable for X-ray structure analysis were obtained by vapor diffusion of diethyl ether into resulting solution over the period of several days. The diffraction data were collected either on a Bruker SMART or a Rigaku R-AXIS RAPID IP X-Ray diffractometer using a graphite monochromator with Mo- $\text{K}\alpha$ radiation ($\lambda = 0.071073$ nm) at 298 or 293K. The structures were solved by direct methods and refined by full-matrix least-squares methods on all F^2 data (SHELX-97)^{S1}.

EPR spectrum measurements: EPR spectra of related two-electron reduction of azo-1,8-naphthyridine were recorded on Bruker E-300, EPR setting as follow: Mod. Frequency: 100 KHz; Microwave power: 10 mW; Modulation amplitude: 0.413 G; Receiver gain: 1.00e+005; Sweep width: 100 G; Scan time: 167.722 s. ERP spectra of related one-electron reduction of azo-pyridine were recorded on Bruker E-500, EPR setting as follow: Mod. Frequency: 100 KHz; Microwave power: 10 mW; Modulation amplitude: 1e-05; Time constant: 0.04096 s; Receiver gain: 50; Microwave frequency: 9.781815e+09 Hz.

Geometry optimization and energy computation: All calculations were performed on the density functional theory (DFT) level using a B3LYP/6-31G(d) basis set, employing the Gaussian 03 suit of programs.^{S2}

Cyclic voltammetric experiment: Cyclic voltammetric experiment was performed using a computer-controlled CHI660C electrochemical workstation with a

conventional three electrode system comprised of platinum as counter electrode, mercury-coated glassy carbon working electrode and saturated calomel electrode as the reference. The experiment was carried out under a nitrogen atmosphere in dimethylformamide solution containing **L** (3.0×10^{-4} mol/L) and $n\text{-Bu}_4\text{NPF}_6$ (5.0×10^{-2} mol/L).

2. Synthesis

Synthesis and characterization of (E)-1,2-bis(5,7-dimethyl-1,8-naphthyridin-2-yl)diazene (L): The new ligand was synthesized by a modification of the literature method using oxidative coupling of 2,4-dimethyl-7-amino-1,8-naphthyridine^{S3} with 10% NaOCl.^{S4} A 100 mL aliquot of a cold solution of 2,4-dimethyl-7-amino-1,8-naphthyridine (4.3 g, 2.48 mmol) in water was added dropwise to 150 mL 10% NaOCl solution. The mixture was stirred at 5-10 °C for 1 h. The resulting solution was then extracted three times with dichloromethane (3×100 mL), and the combined extracts were dried over anhydrous sodium sulfate were evaporated until dry in vacuo, leaving an orange solid. The crude product was purified by column chromatography over Al_2O_3 (100-200 mesh with $\text{CHCl}_3/\text{CH}_3\text{CH}_2\text{OH}$ (v/v, 100/1) as eluent). Yield: 70%. Mp: decomposed above 200 °C without melting. ¹H NMR (500 MHz, $\text{DMSO}-d_6$) δ (ppm): 2.74 (s, 3H, 4-Me of naphthyridine ring), 2.76 (s, 3H, 2-Me of naphthyridine ring), 7.55 (s, 1H, naphthyridyl proton at 3-position), 8.05 (d, $J = 8.8$ Hz, 1H, naphthyridyl proton at 5-position), 8.87 (d, $J = 8.7$ Hz, 1H, naphthyridyl proton at 6-position); ¹³C NMR (400 MHz, $\text{CDCl}_3/\text{CD}_3\text{OD}$ 10/1) δ (ppm): 18.3, 25.5, 110.7, 122.9, 125.0, 136.4, 145.8, 155.3, 163.4, 164.2; Anal. Calc. for $\text{C}_{20}\text{H}_{18}\text{N}_6$: C, 70.16; H, 5.30; N, 24.54. Found: C, 69.78; H, 5.40; N, 24.82%. MALDI-TOF MS: m/z 343 ($\text{M}+\text{H}$)⁺.

Synthesis and characterization of the octanuclear Zn(II) complex (I) $\text{Zn}_8(\text{L})_2(\text{O})_2(\text{OAc})_8$: The ligand **L** (56 mg, 0.16 mmol) and $\text{Zn}(\text{OAc})_2 \cdot 2\text{H}_2\text{O}$ (140.5 mg, 0.64 mmol) were suspended in 30 mL of a $\text{CH}_2\text{Cl}_2/\text{CH}_3\text{OH}$ (v/v, 10/1) mixed solvent under nitrogen atmosphere, the mixture was stirred at ambient temperature for 24 h. Diethyl ether was added to the resulting solution to give the purple precipitation; the crude product was isolated by suction filtration and recrystallized. The dark red crystals suitable for X-ray diffraction were obtained by diffusion of diethyl ether into a dichloromethane solution. Yield: 84%. ¹H NMR (400 MHz, $\text{CDCl}_3/\text{CD}_3\text{OD}$ 10/1) δ (ppm): 2.00 (s, 9H, Me of acetyl), 2.49 (s, 3H, 4-Me of naphthyridyl ring), 2.64 (s, 3H,

2-Me of naphthyridyl ring), 6.71 (s, 1H, naphthyridyl proton at 3-position), 7.18 (d, $J = 9.5$ Hz, 1H, naphthyridyl proton at 5-position), 7.53 (d, $J = 9.6$ Hz, 1H, naphthyridyl proton at 6-position). ^{13}C NMR (400 MHz, $\text{CDCl}_3/\text{CD}_3\text{OD}$ 10/1) δ (ppm): 18.8, 19.6, 22.3, 117.9, 122.1, 129.9, 149.9, 150.3, 151.8, 156.6, 180.3. Anal. Calc. for $\text{C}_{56}\text{H}_{60}\text{N}_{12}\text{O}_{18}\text{Zn}_8$ (powders): C, 39.28; H, 3.53; N, 9.82. Found: C, 38.87; H, 3.30; N, 10.05%.

Synthesis and characterization of 1,2-bis(5,7-dimethyl-1,8-naphthyridin-2-yl)hydrazine (H_2L): The compound was synthesized by direct reduction of the azo-1,8-naphthyridine. **L** (2 g, 5.8 mmol) in 200 mL of acetic acid was stirred at ambient temperature over a night, neutralized with $\text{NH}_3 \cdot \text{H}_2\text{O}$ in ice bath to pH = 8. The resulting solution was then extracted three times with dichloromethane (3×200 mL), the organic phase were combined and dried over anhydrous sodium sulfate. After filtration and removal of the solvent under reduced pressure, the crude product was purified by chromatography on Al_2O_3 (silica gel 100-200 mesh with $\text{CH}_2\text{Cl}_2/\text{CH}_3\text{OH}$ (v/v, 20/1) as eluent). Red crystal was obtained by slow vaporation of the compound in chloroform solution. Yield: 75%. Mp: above 250 °C. ^1H NMR (300 MHz, CD_2Cl_2) δ (ppm): 2.38 (s, 6H, 4-Me of naphthyridyl ring), 2.42 (s, 6H, 2-Me of naphthyridyl ring), 6.54 (d, $J = 9.7$ Hz, 2H, naphthyridyl proton), 6.66 (s, 2H, naphthyridyl proton), 7.27 (d, $J = 9.6$ Hz, 2H, naphthyridyl proton), 9.55 (br, 2H, active proton of imino); ^{13}C NMR (500 MHz, $\text{CDCl}_3/\text{CD}_3\text{OD}$ 10/1) δ (ppm): 17.85, 24.28, 110.61, 113.14, 119.00, 121.61, 124.71, 128.33, 136.00, 144.14, 149.97, 158.08; Anal. Calc. for $\text{C}_{20}\text{H}_{20}\text{N}_6$ (powders): C, 69.75; H, 5.85; N, 24.40. Found: C, 69.53; H, 5.84; N, 24.63%. MALDI-TOF MS: m/z 345 ($\text{M}+\text{H}$) $^+$.

Synthesis and characterization of the tetranuclear Zn^{II} complex (2**) $\text{Zn}_4(\text{L1})_2(\text{OH})(\text{OMe})(\text{OAc})_4$:** The ligand **L1**^{S5} (43 mg, 0.18 mmol) and $\text{Zn}(\text{OAc})_2 \cdot 2\text{H}_2\text{O}$ (157.1 mg, 0.72 mmol) were suspended in 30 mL of a $\text{CH}_2\text{Cl}_2/\text{CH}_3\text{OH}$ (v/v, 10/1) mixed solvent under nitrogen atmosphere, the mixture was stirred at ambient temperature for 24 h. The dark brown crystal was obtained following the same procedure as **1** except that **L1** was used. Yield: 60%. The hydroxyl group and methyl group of **2** were disordered over two distinct sites and their occupancies were 50%, respectively, which results in the lack of hydrogen bonding involving the hydroxyl group in the crystal lattice of **2**. ^1H NMR (400 MHz, CDCl_3) δ (ppm): 1.67 (s, 6H, Me of acetyl and pyridine ring), 2.04 (s, 18H, Me of acetyl and

pyridine ring), 2.72 (s, 3H, Me of MeO), 7.32 (m, 1H, pyridyl proton at 4-position), 7.78-7.79 (m, 2H, pyridyl proton). IR (KBr, cm^{-1}): 1591.5, 1559.4, 1459.9, 1321.2, 1261.3, 1168.3. Anal. Calc. for $\text{C}_{33}\text{H}_{40}\text{N}_8\text{O}_{10}\text{Zn}_4$: C, 40.85; H, 4.16; N, 11.55. Found: C, 41.31; H, 4.32; N, 11.36%. ESI MS m/z : $(\text{M}+2\text{H})^{2+}$ 486.2 .

References

- S1. G. M. Sheldrick, *SHELX-97, Program for the Refinement of Crystal Structures*, University of Göttingen, Germany, 1997.
- S2. M. J. Frisch, G. W. Trucks, H. B. Schlegel, G. E. Scuseria, M. A. Robb, J. R. Cheeseman, J. A., Jr. Montgomery, T. Vreven, K. N. Kudin, J. C. Burant, J. M. Millam, S. S. Iyengar, J. Tomasi, V. Barone, B. Mennucci, M. Cossi, G. Scalmani, N. Rega, G. A. Petersson, H. Nakatsuji, M. Hada, M. Ehara, K. Toyota, R. Fukuda, J. Hasegawa, M. Ishida, T. Nakajima, Y. Honda, O. Kitao, H. Nakai, M. Klene, X. Li, J. E. Knox, H. P. Hratchian, J. B. Cross, C. Adamo, J. Jaramillo, R. Gomperts, R. E. Stratmann, O. Yazyev, A. J. Austin, R. Cammi, C. Pomelli, J. W. Ochterski, P. Y. Ayala, K. Morokuma, G. A. Voth, P. Salvador, J. J. Dannenberg, V. G. Zakrzewski, S. Dapprich, A. D. Daniels, M. C. Strain, O. Farkas, D. K. Malick, A. D. Rabuck, K. Raghavachari, J. B. Foresman, J. V. Ortiz, Q. Cui, A. G. Baboul, S. Clifford, J. Cioslowski, B. B. Stefanov, G. Liu, A. Liashenko, P. Piskorz, I. R. Komaromi, L. Martin, D. J. Fox, T. Keith, M. A. Al-Laham, C. Y. Peng, A. Nanayakkara, M. Challacombe, P. M. W. Gill, B. Johnson, W. Chen, M. W. Wong, C. Gonzalez and J. A. Pople, *Gaussian 03*, Revision B.05; Gaussian, Inc.: Pittsburgh, PA, 2003.
- S3. R. A. Henry and P. R. Hammond, *J. Heterocyclic Chem.*, 1977, **14**, 1109.
- S4. J. P. Launay, M. Tourrel-Pagis, J. F. Lipskier, V. Marvaud and C. Joachim, *Inorg. Chem.*, 1991, **30**, 1033.
- S5. The ligand **L1** was synthesized according to this published procedures, using 6-methyl-2-aminepyridine instead of 2-aminepyridine, see S3, S4.

Table1. Summary of X-ray Crystallographic Data for Compounds **1**, **2**, **L** and **H₂L**.

compounds	1 ·2CH ₂ Cl ₂	2	L	H₂L ·2CHCl ₃
formula	C ₂₉ H ₃₂ Cl ₂ N ₆ O ₉ Zn ₄	C ₃₃ H ₄₀ N ₈ O ₁₀ Zn ₄	C ₂₀ H ₁₈ N ₆	C ₁₁ H ₁₁ Cl ₃ N ₃
fw	940.99	970.21	342.40	291.58
space group	C2/c	P2(1)/c	P2(1)/n	P2(1)/n
cryst syst	monoclinic	monoclinic	monoclinic	monoclinic
<i>a</i> (Å)	22.926(3)	11.350(2)	8.017(4)	7.338(2)
<i>b</i> (Å)	12.283(2)	17.192(2)	10.788(6)	22.678(5)
<i>c</i> (Å)	26.975(3)	10.065(2)	10.389(6)	8.087(2)
<i>α</i> (deg)	90	90	90	90
<i>β</i> (deg)	104.015(2)	99.210(2)	96.298(7)	95.07(3)
<i>γ</i> (deg)	90	90	90	90
<i>V</i> (Å ³)	7370(2)	1938.7(5)	893.0(9)	1340.5(5)
<i>Z</i>	8	2	2	4
<i>T</i> (K)	298(2)	298(2)	298(2)	293(2)
<i>ρ</i> _{calcd} (g cm ⁻³)	1.696	1.662	1.273	1.445
<i>θ</i> _{rang} (deg)	1.56-25.01	1.82-25.00	2.73-24.99	2.68-25.03
<i>μ</i> (mm ⁻¹)	2.774	2.510	0.080	0.664
crystal size (mm)	0.21×0.12×0.05	0.46×0.31×0.18	0.56×0.41×0.25	0.40×0.35×0.12
GOF	0.886	1.043	1.020	0.931
no. of unique data	6509	3397	1575	2318
no. of parameters	564	278	118	155
<i>R</i> _{int}	0.0876	0.0327	0.0596	0.0347
<i>R</i> _{<i>I</i>} ^{<i>a</i>}	0.0526	0.0457	0.0587	0.0551
<i>wR</i> ₂ ^{<i>a</i>}	0.0967	0.1106	0.1536	0.1204
max, min peaks (e Å ⁻³)	0.626, -0.564	0.743, -0.288	0.499, -0.141	0.200, -0.247

$$^a I > 2\sigma(I). R_I = \frac{\sum ||F_o| - |F_c||}{\sum |F_o|}. wR_2 = \left\{ \frac{\sum [w(F_o^2 - F_c^2)^2]}{\sum [w(F_o^2)]} \right\}^{1/2}$$

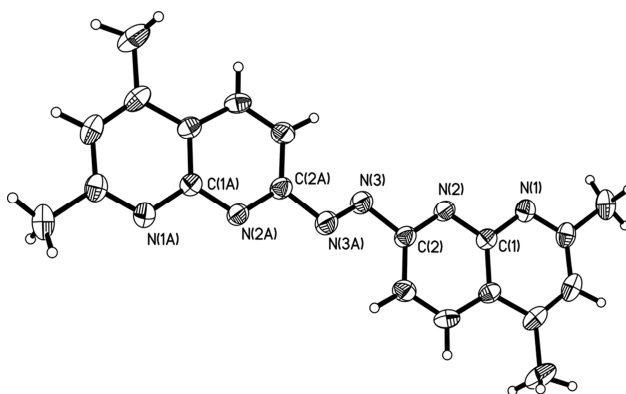


Fig. S1. A perspective view of **L** representing the thermal ellipsoids with 30% probabilities.

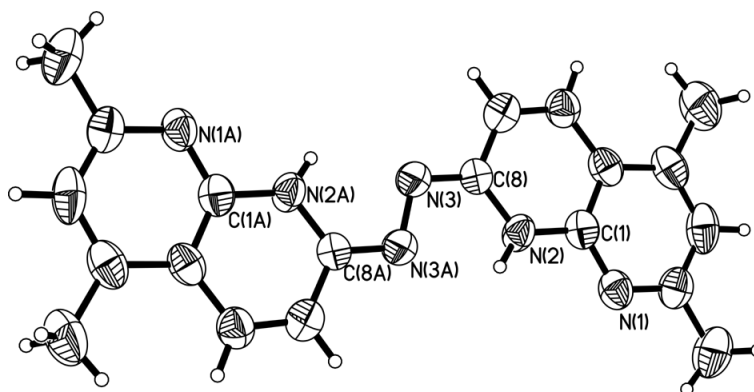


Fig. S2. A perspective view of **H₂L** representing the thermal ellipsoids with 30% probabilities.

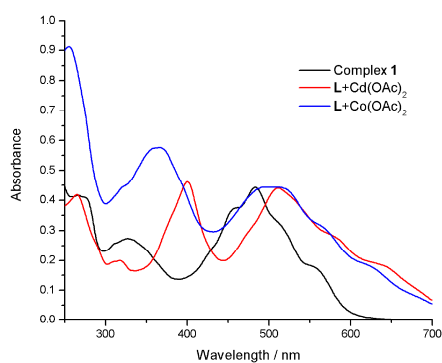


Fig. S3. UV-Vis absorption spectra of complex **1** in CH₂Cl₂ solution (black line); **L** and Cd(OAc)₂•2H₂O in CH₂Cl₂/CH₃OH mixed solution after reaction for 20 h (red line), **L** and Co(OAc)₂•4H₂O after reaction for 3.5 h (blue line) in CH₂Cl₂/CH₃OH mixed solution at room temperature.



Fig. S4. Comparison with those of Fig. 3a in the presence of DMPO in the text, EPR spectral signals were not observed during reaction of **L** (5.5×10^{-3} M) and NaOAc (1.1×10^{-2} M) in the absence of DMPO in N_2 -saturated CH_3OH/CH_2Cl_2 (v/v, 1/1) solution at 298K ($V_L/V_{Zn(OAc)_2} = 1:4$).

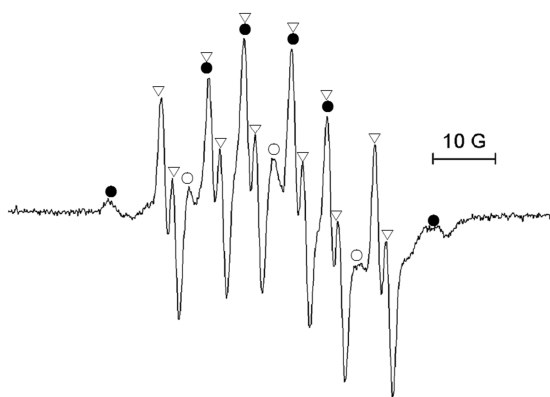


Fig. S5. EPR spectra observed during reaction of **L** (5.5×10^{-3} M) and $Cd(OAc)_2 \cdot 2H_2O$ (5.5×10^{-3} M) in N_2 -saturated CH_3OH/CH_2Cl_2 (v/v, 1/1) solution ($V_L/V_{Cd(OAc)_2} = 1:4$, DMPO = 0.2 M) at 298K. ● DMPO/ $\bullet CH_3$ ($a_N = 15.60 \pm 0.1$ G, $a_H = 23.56 \pm 0.1$ G), ▽ DMPO/acyloxy radical ($a_N = 13.58 \pm 0.1$ G, $a_{H\beta} = 7.79 \pm 0.1$ G, $a_{H\gamma} = 1.79 \pm 0.1$ G), the signals marked with ○ are due to DMPO decomposition.

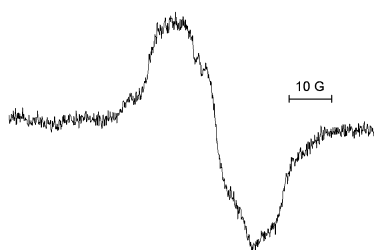


Fig. S6. EPR spectra observed during reaction of **L** (5.5×10^{-3} M) and $Cd(OAc)_2 \cdot 2H_2O$ (5.5×10^{-3} M) in N_2 -saturated CH_3OH/CH_2Cl_2 (v/v, 1/1) solution ($V_L/V_{Cd(OAc)_2} = 1:4$, $g = 2.0059$) at 298K.

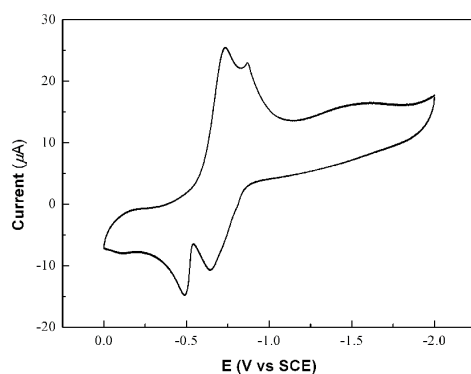


Fig. S7. Cyclic voltammogram of **L** under a nitrogen atmosphere in dimethylformamide solution containing **L** (3.0×10^{-4} mol/L) and TBAPF₆ (5.0×10^{-2} mol/L) at a scan rate of 100 mV/s.

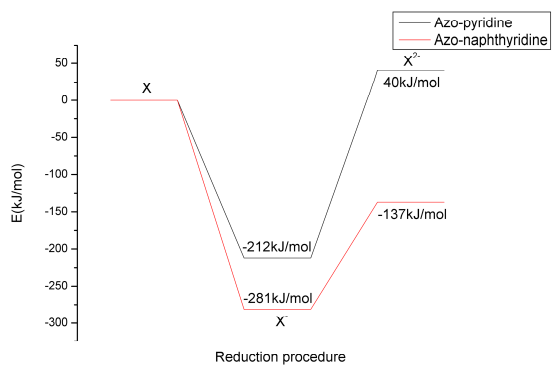


Fig. S8. Energy of azo-1,8-naphthyridine and azo-pyridine changes during reduction process calculated by a geometry optimization and energy computation based on B3LYP/6-31G(d).

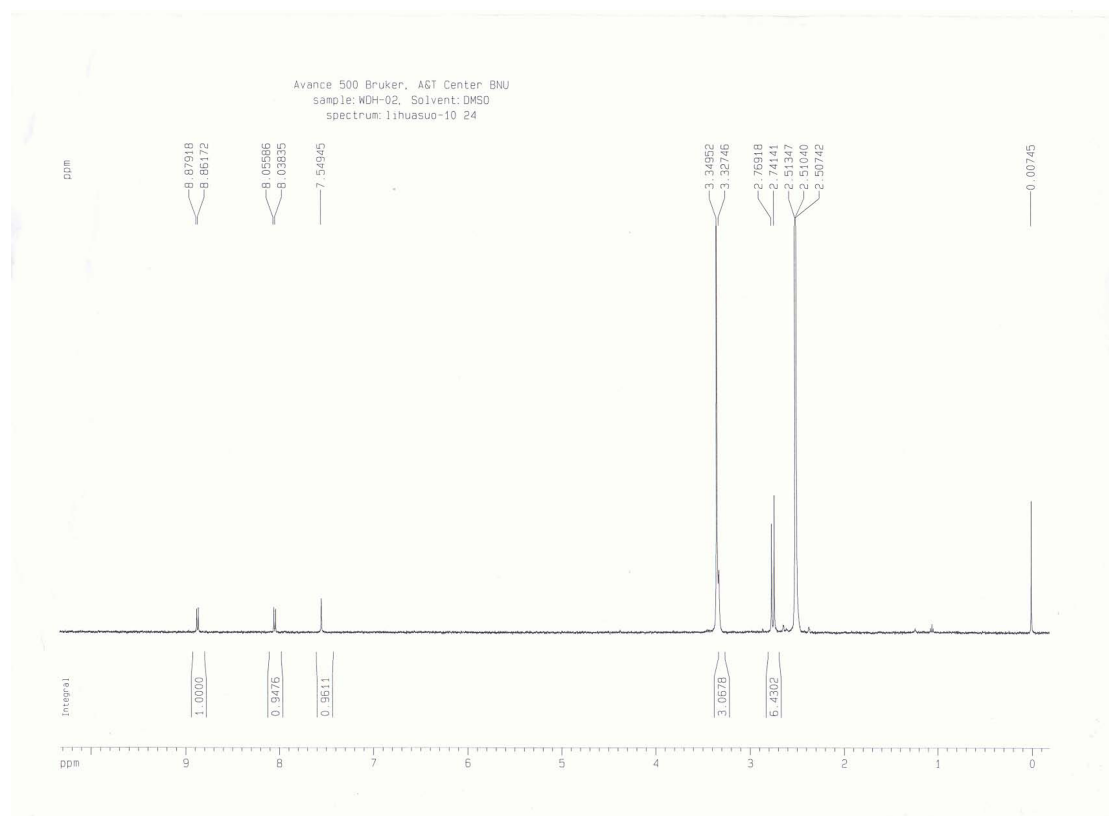


Fig. S9. ^1H NMR spectrum of L at 298 K in $\text{DMSO-}d_6$.

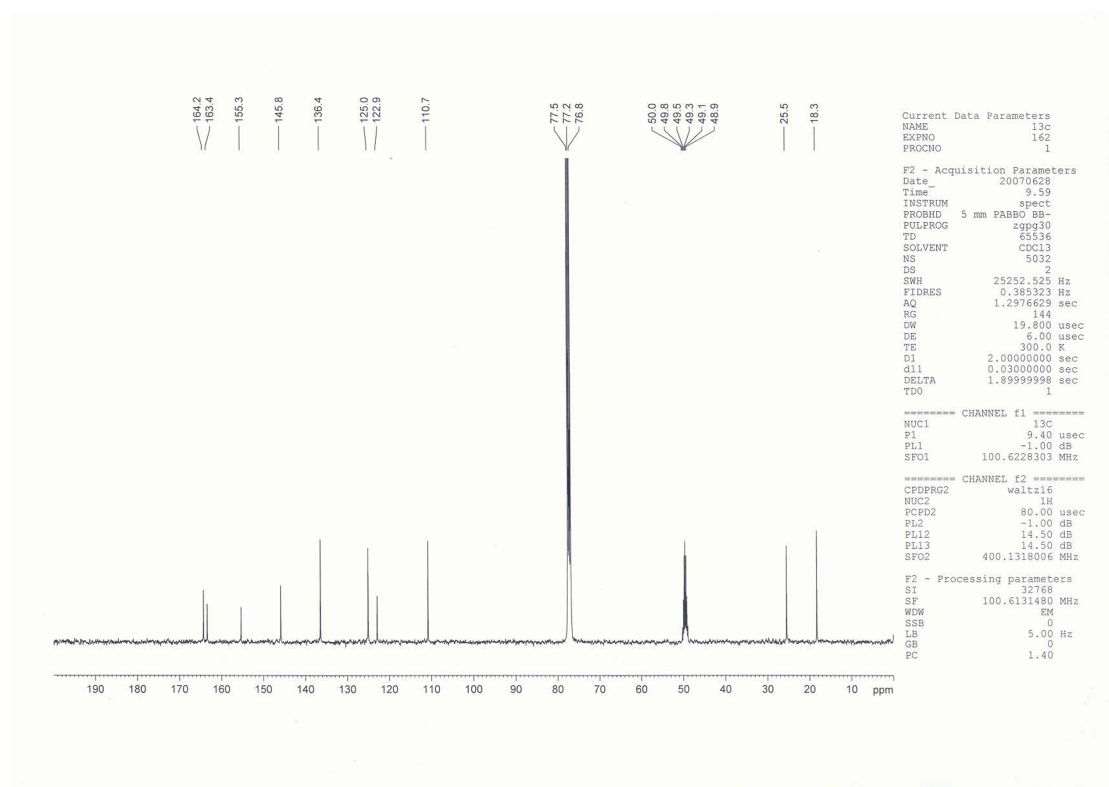


Fig. S10. ^{13}C NMR spectrum of L at 298 K in $\text{CDCl}_3/\text{CD}_3\text{OD}$ (v/v, 10/1).

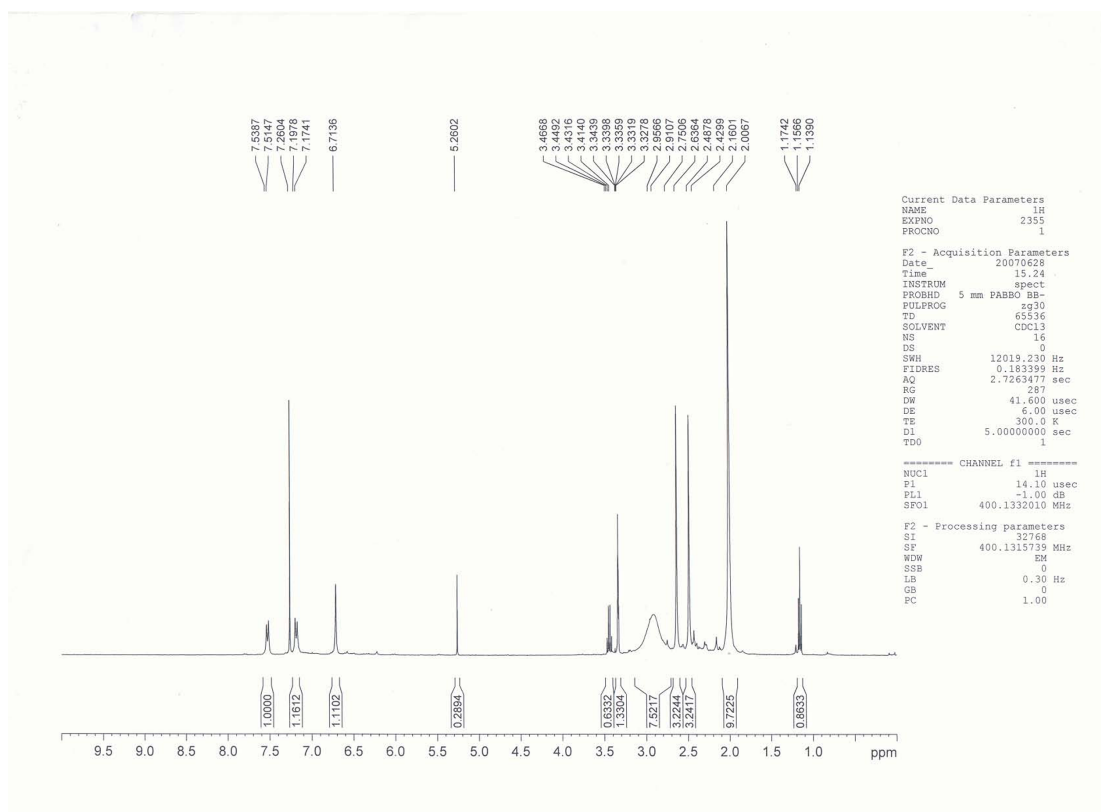


Fig. S11. ^1H NMR spectrum of complex **1** at 298 K in $\text{CDCl}_3/\text{CD}_3\text{OD}$ (v/v, 10/1).

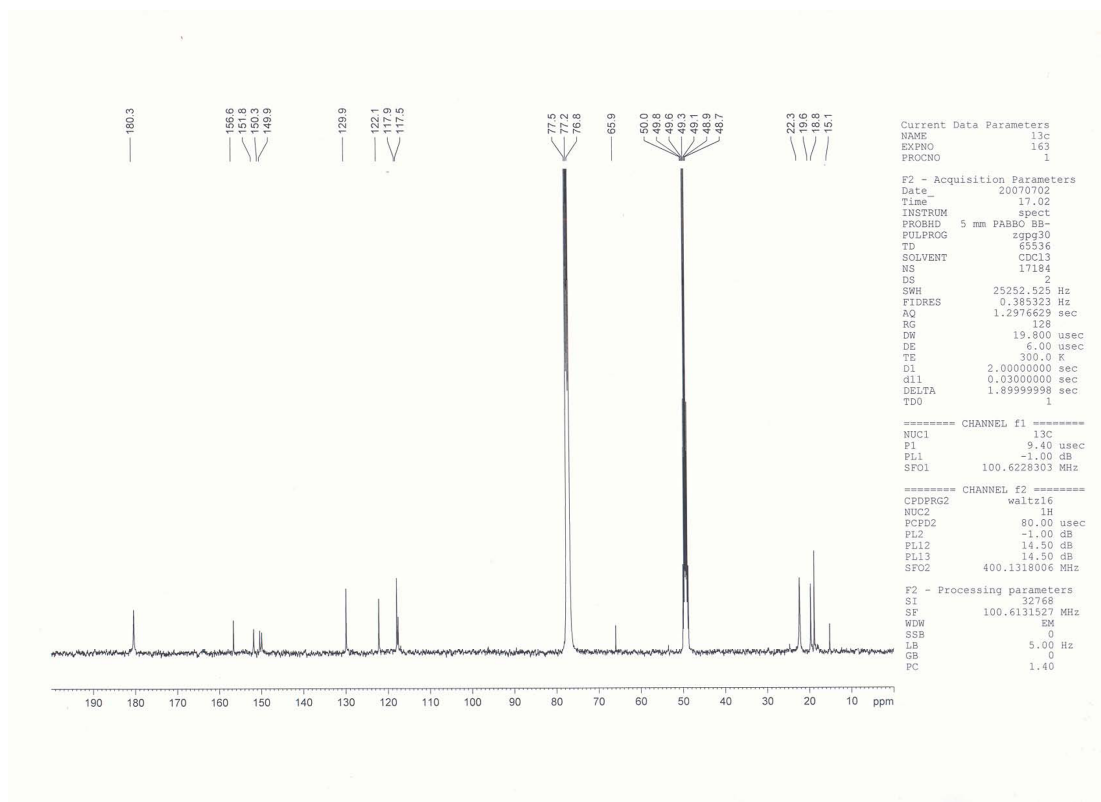


Fig. S12. ^{13}C NMR spectrum of complex **1** at 298 K in $\text{CDCl}_3/\text{CD}_3\text{OD}$ (v/v, 10/1).

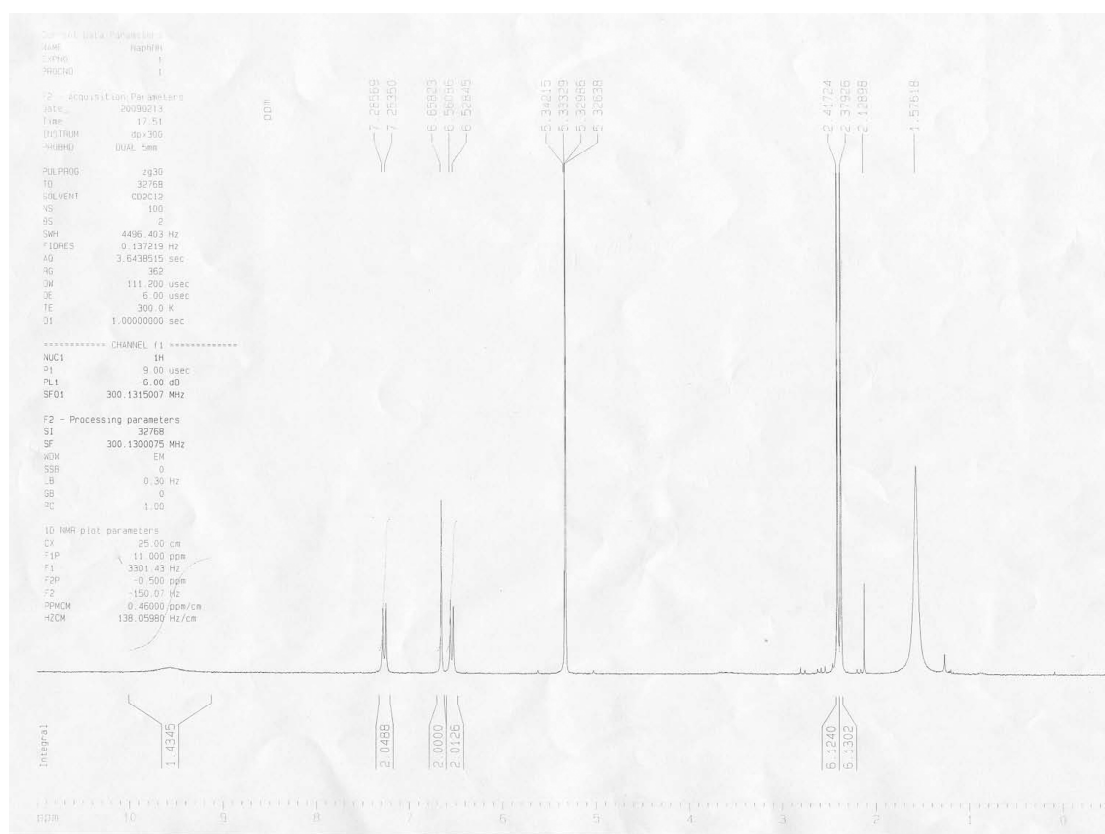


Fig. S13. ^1H NMR spectrum of H_2L at 298 K in CD_2Cl_2 .

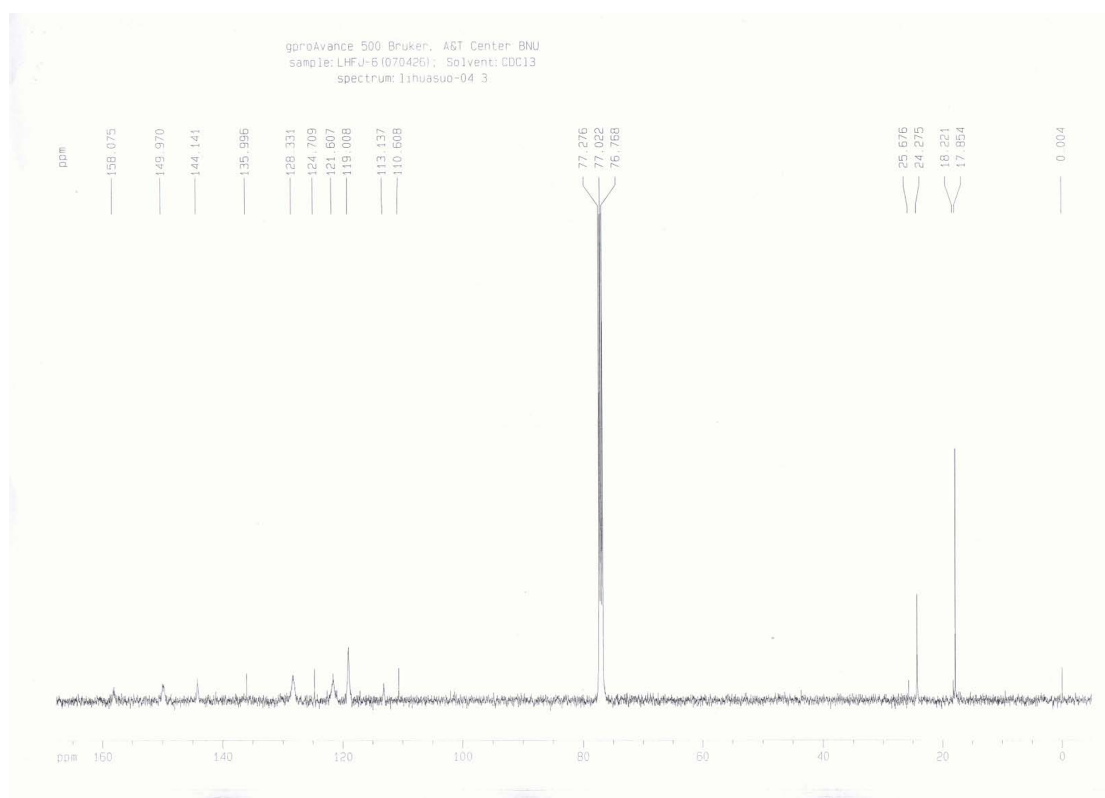


Fig. S14. ^{13}C NMR spectrum of H_2L at 298 K in $\text{CDCl}_3/\text{CD}_3\text{OD}$ (v/v, 10/1).

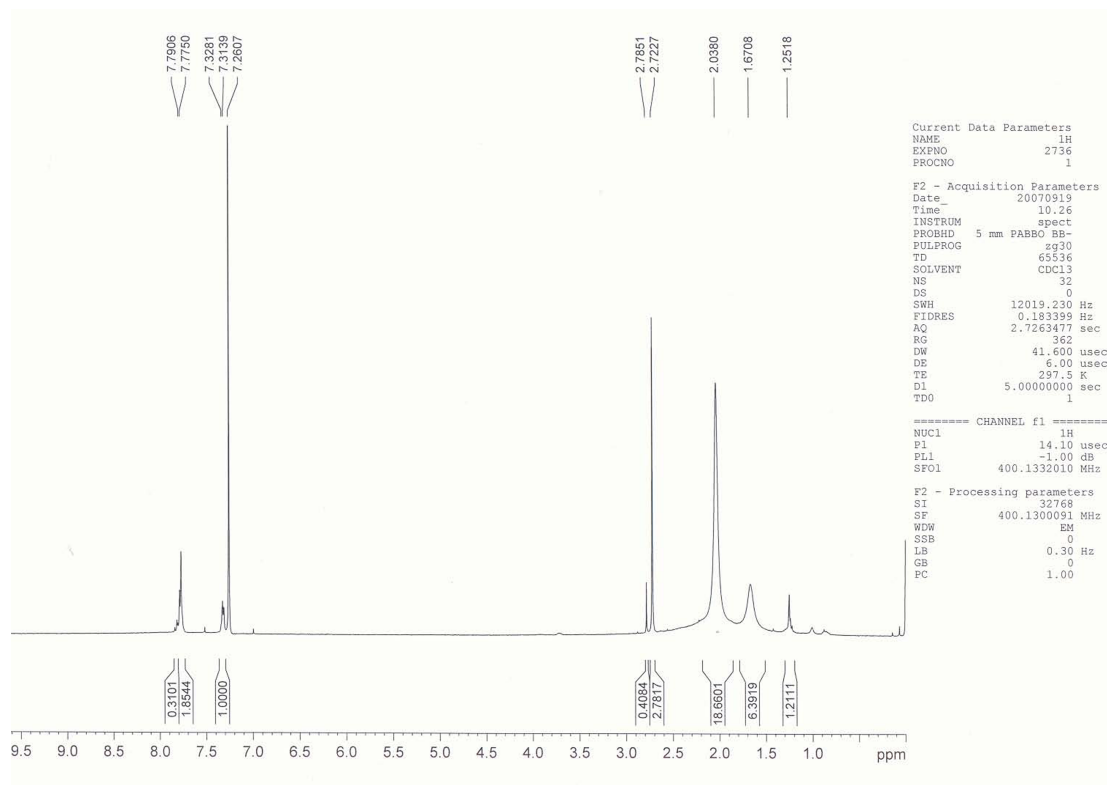


Fig. S15. ^1H NMR spectrum of complex **2** at 298 K in CDCl_3 .

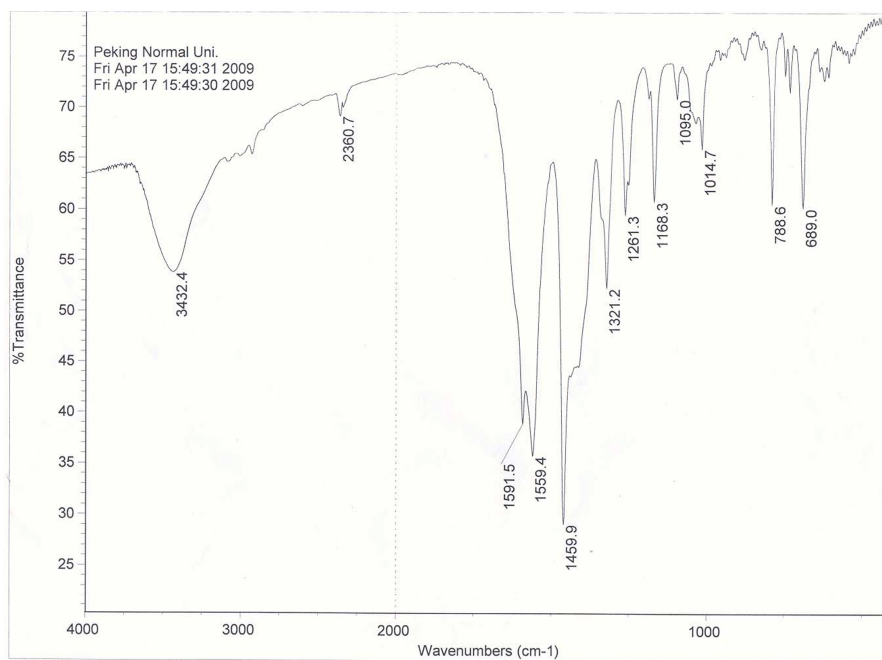


Fig. S16. IR spectrum of **2** at 298 K.

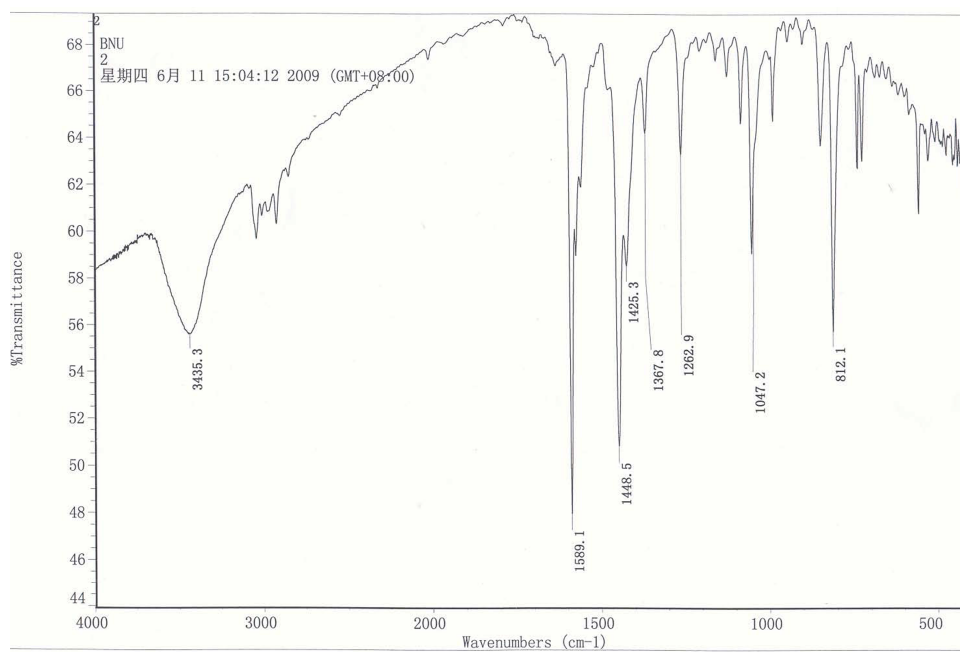


Fig. S17. IR spectrum of L1 at 298 K.